RESEARCH ARTICLE

The neuroprotective role of microglial cells against amyloid beta-mediated toxicity in organotypic hippocampal slice cultures

Maren Richter[1,2]*; Natascha Vidovic[1,3]* ; Knut Biber[4,5]; Amalia Dolga[2,6] ; Carsten Culmsee[2] ; Richard Dodel[1,3]*

[1] Department of Neurology, Philipps-University Marburg, Marburg, Germany.
[2] Institute for Pharmacology and Clinical Pharmacy, Philipps-University Marburg, Marburg, Germany.
[3] Chair of Geriatric Medicine, University Duisburg-Essen, Essen, Germany.
[4] Molecular Psychiatry, Psychiatric Hospital, University of Freiburg, Freiburg, Germany.
[5] Department of Neuroscience, University Medical Center Groningen, University of Groningen, Groningen, the Netherlands.
[6] Department of Molecular Pharmacology, Groningen Research Institute of Pharmacy, Faculty of Science and Engineering, Groningen, the Netherlands.

Abstract

During Alzheimer's disease (AD) progression, microglial cells play complex roles and have potentially detrimental as well as beneficial effects. The use of appropriate model systems is essential for characterizing and understanding the roles of microglia in AD pathology. Here, we used organotypic hippocampal slice cultures (OHSCs) to investigate the impact of microglia on amyloid beta (Aβ)-mediated toxicity. Neurons in OHSCs containing microglia were not vulnerable to cell death after 7 days of repeated treatment with $A\beta_{1-42}$ oligomer-enriched preparations. However, when clodronate was used to remove microglia, treatment with $A\beta_{1-42}$ resulted in significant neuronal death. Further investigations indicated signs of endoplasmic reticulum stress and caspase activation after $A\beta_{1-42}$ challenge only when microglia were absent. Interestingly, microglia provided protection without displaying any classic signs of activation, such as an amoeboid morphology or the release of pro-inflammatory mediators (e.g., IL-6, TNF-α, NO). Furthermore, depleting microglia or inhibiting microglial uptake mechanisms resulted in significant more Aβ deposition compared to that observed in OHSCs containing functional microglia, suggesting that microglia efficiently cleared Aβ. Because inhibiting microglial uptake increased neuronal cell death, the ability of microglia to engulf Aβ is thought to contribute to its protective properties. Our study argues for a beneficial role of functional ramified microglia whereby they act against the accumulation of neurotoxic forms of Aβ and support neuronal resilience in an *in situ* model of AD pathology.

INTRODUCTION

Existing data strongly suggest that inflammatory processes contribute to Alzheimer's disease (AD) pathology (36). However, microglial cells, the innate immune cells of the brain, seem to play complex roles in the progression of AD, wherein they may exert both neurotoxic and neuroprotective properties (14). *In vitro* data indicate that fibrils and soluble Aβ oligomers bind to various microglial surface receptors, resulting in a pro-inflammatory response of the cells (58). Pro-inflammatory microglia are thought to have a direct neurotoxic effect by releasing detrimental compounds, including reactive oxygen species (ROS) and nitric oxide (NO) (61). Recent data indicate that microglia activation patterns are highly variable and that the pro-inflammatory activity is only one possible response phenotype of microglia (21, 30, 50). In post mortem analyses of AD patients' brains,

microglia were found to surround amyloid beta (Aβ) plaques (34, 77). In addition, *in vitro* studies have demonstrated that microglia engulf Aβ fibrils via receptor-mediated phagocytosis (64) and degrade soluble oligomers either through pinocytosis (64) or by secreting Aβ-degrading enzymes, such as neprilysin and insulin-degrading enzyme (58). Nevertheless, it remains unknown whether microglial uptake of Aβ affects neurodegeneration in AD pathology. Besides, accumulation of misfolded proteins inside the ER lumen and the formation of toxic products, including ROS, are supposed to result in activation of stress responses in the endoplasmic reticulum (ER stress) (10). In AD, several human studies provide evidence for an involvement of ER stress in disease progression (39, 40, 59, 75). Various ER stress-related proteins have been shown to be upregulated in AD patients' brains. The increased levels of folding proteins like 78 kDa glucose regulating protein (GRP78) and ER stress-specific caspase cleavage were

also found in AD *post mortem* brains (70). Organotypic hippocampal slice cultures (OHSCs) are regarded as an excellent model system for investigating glia–neuron interplay in the context of AD-related neurodegeneration because such cultures preserve *in vivo* morphology and activity of all cell types present in the hippocampal region (45, 88). Microglia in general can appear in different morphological shapes with distinct functions. These activation states are said to be reversible (67) making them highly adaptive and able to react to environmental changes. Under healthy conditions, microglial cells display a "ramified" morphology and function as the brain's controlling unit (17, 73). Thereby they are not "inactive." Ceaselessly, with their long processes they are scanning the surrounding for invaders and pathogens or aggregated misfolded proteins (35, 49, 72). In conditions of inflammation or damage, they adapt an activation state formerly referred to as M1 or M2, respectively (1, 73), but in 2015, Schultze and colleagues proposed a more diverse activation pattern of microglia which can react to various "input signals" as it is not all black and white (76). In contrast to pure, isolated microglial cultures that display various morphologies ranging from needle-like to amoeboid in shape, in OHSCs, microglia maintain their natural environment and therefore show a predominately ramified morphology (33, 88). In addition, neurons in slice cultures have intact synapses with an *in vivo*-like distribution of receptors (e.g., NMDA receptors) that results in drug sensitivity and EC_{50} values similar to those observed in living organisms (38). OHSCs are therefore an ideal tool to investigate the function of microglia in an *in vivo*-like cellular environment (33, 65).

In the present study, we used OHSCs to examine the impact of microglial cells on Aβ-mediated effects. Neuronal death induced by treatment with Aβ, and the mechanisms underlying were characterized in the presence or absence of microglia.

MATERIALS AND METHODS

Preparation and cultivation of OHSCs

The preparation of organotypic hippocampal slice cultures was performed as previously described (79), with minor modifications. Postnatal day 1–4 C57Bl/6J mice (Janvier, Le Genest-saint-Isle, France or Charles River Laboratories, Sulzfeld, Germany) were sacrificed by decapitation, and their brains were dissected. Hippocampi were dissected, cut into 375-µm thick slices using a McIlwain tissue chopper (Mickle laboratory engineering, Surrey, UK) and cultivated on membrane inserts (Millicell cell culture inserts, 0.4 µm pore size, Merck Millipore, Darmstadt, Germany) in 6-well plates. Per well, six slices were arranged on a membrane insert, with each well containing 1.2 mL sterile-filtered (Whatman syringe filters, 0.2 µm pore size PES, Merck, Darmstadt, Germany) culture medium (for 100 mL: 41.6 mL *aqua ad injectabilia*, 5 mL Minimum Essential Medium 10×, 25 mL Basal Eagle's + Earle's Medium, 25 mL HyClone Donor Equine Serum, 1 mL GlutaMax, 1.44 mL 45% glucose solution, pH 7.2; all life

technologies, Carlsbad, USA), The hippocampal slices were incubated in a humidified atmosphere containing 5% CO_2 at 35°C.

To specifically deplete microglia, 100 µg/mL clodronate disodium salt (Merck Millipore, Darmstadt, Germany) was added to the medium, as previously described (54). The day after preparation, slices were washed with 1× PBS (Merck Millipore, Darmstadt, Germany), and inserts were transferred into a new 6-well plate containing fresh culture medium without clodronate. Culture medium was changed every 2–3 days, and treatment started 6–7 days after preparation.

Amyloid beta (Aβ$_{1-42}$) application to OHSCs

The preparation of Aβ$_{1-42}$ oligomer-enriched solutions was performed as previously described (23). A total of 1 mg Aβ$_{1-42}$ (Bachem, Bubendorf, Switzerland) were dissolved in 10% ammonia (Sigma-Aldrich, Taufkirchen, Germany) to a final concentration of 1 mg/mL and then aliquoted into low-binding tubes (Eppendorf, Hamburg, Germany). Afterward, the aliquots were freeze-dried to obtain 25 µg protein and stored at −80°C until use. Before used in OHSCs, Aβ$_{1-42}$ aliquots were dissolved in *aqua ad injectabilia* (1 mg/mL) and filled up with 100 mM Tris, 50 mM NaCl (Sigma-Aldrich, Taufkirchen, Germany), pH 7.4, to obtain a 58 µM solution. As a negative control, the described Tris/NaCl buffer was prepared without adding Aβ$_{1-42}$ peptide. The Aβ$_{1-42}$ solution and the solution containing the buffer without the peptide were each stirred for 48 h at 1400 rpm at room temperature. For the treatment of OHSCs, 2 µL of the freshly prepared oligomer-enriched 58 µM Aβ$_{1-42}$ solution was dropped on top of each of the slices, considering six slices per well containing 1.2 mL culture medium; the final concentration of Aβ$_{1-42}$ is 0.6 µM. To obtain higher concentrations, oligomeric Aβ$_{1-42}$ solution additionally was applied on top of the slices at a concentration of 1 µM (3 µL per slice), to obtain a final concentration of 1.6 µM in the well. It is not recommended to add more than 3 µL of solution at once on top of the slices because the excess liquid will slide off and end up in the media too quickly. To obtain lower (0.3 µM) concentrations of Aβ$_{1-42}$, the stock solution (58 µM) was diluted in culture medium to 30 µM, and then, 2 µL of this dilution was dropped on top of the slices to obtain a final concentration of 0.3 µM in the well. By dropping Aβ$_{1-42}$ directly on top of the slices, it is more likely to be taken up and interacts with the cells than by adding it to the media. The Aβ$_{1-42}$ peptide was re-applied on top of the slices with every media change, which occurred 3 times over one week.

Detection of neuronal cell death

Propidium iodide (PI) staining was performed with immunostaining to detect neuronal cell death in OHSCs. Following Aβ$_{1-42}$ treatment, PI was added to the medium at a final concentration of 10 µg/mL, and the cultures were incubated for 1 h at 35°C. Afterward, the dye was removed, and the OHSCs were washed and fixated in 4% paraformaldehyde (PFA) solution. After several washes,

immunostaining was performed for neurons (NeuN) and microglial cells (Iba1). ImageJ (Rasband, W.S., ImageJ, U. S. National Institutes of Health, Bethesda, MD, USA) was used to analyze neuronal cell death in OHSCs. An oval selection tool was used for the hippocampal regions (CA1+3 and DG). The threshold was adjusted for far-red (Iba-1), red (PI) and green (NeuN). The area covered with far-red (Iba-1), red (PI) and green (NeuN) within the selected oval area was measured. Only slices with less than 10% of the hippocampus regions CA1+3 and DG covered with Iba1-positive microglia were used for quantification of cell death. Therefore, the microglial presence was calculated by dividing the magenta area (Iba-1) by the green area (NeuN). Neuronal cell death within one hippocampal slice was calculated as the red area (PI) divided by the green area (NeuN). The presented data were pooled from several hippocampal slice cultures representing three independent experiments per condition.

Detection of activated caspases

CaspACE™ FITC-VAD-FMK (Promega, Madison, USA) was used to detect activated caspases inside the cells. The OHSC culture medium was removed, and medium containing CaspACE™ FITC-VAD-FMK at a final concentration of 5 μM was applied with the $Aβ_{1-42}$ treatment. The cultures were then incubated for 48 h. At the end of the treatment period, the slices were washed, fixed with 4% PFA and immunostained.

ImageJ was used to analyze caspase activation in OHSCs. The oval selection tool was used so select hippocampal regions (CA1+3 and DG). The threshold was adjusted for green (CaspACE™ FITC) and far-red (NeuN), and the areas expressing each color within the selected oval area were measured. Neuronal caspase activity within one hippocampal slice was calculated as the green area divided by the far-red area.

Thioflavin T staining

After respective treatments, the OHSC culture medium was removed from each culture, and the slices were washed in 1× PBS (Merck Millipore, Darmstadt, Germany) and fixed with 4% PFA at 4°C. To stain amyloid deposits, Thioflavin T (ThioT, Sigma-Aldrich, Taufkirchen, Germany) was diluted to a final concentration of 0.1% in *aqua bidest*. A ThioT working solution was mixed 1:1 in 100% ethanol and applied to slices for 10 minutes at RT in the dark. Slices were then washed with 80% ethanol and *aqua bidest*, and the procedure for immunostaining was then performed.

ImageJ was used to analyze ThioT staining in OHSCs. The oval selection tool was used to select hippocampal regions (CA1+3 and DG). After adjustment for the appropriate threshold value, the amount of ThioT within the selected oval area was measured.

Immunocytochemistry

The PFA-fixed slices were cut off from the membrane and transferred into 3% BSA solution for blocking. Afterward, the slices were incubated with primary antibodies (anti-NeuN,

Merck Millipore, Darmstadt, Germany and anti-Iba1, Wako Chemicals GmbH, Neuss, Germany) overnight at 4°C. After the tissues were washed three times for 20 minutes, fluorescently labeled secondary antibodies (all Invitrogen, Karlsruhe, Germany; anti-mouse IgG (H+L) AlexaFluor488, anti-mouse IgG (H+L) AlexaFluor 546, anti-rabbit IgG (H+L) AlexaFluor647, and anti-rabbit IgG (H+L) AlexaFluor546, all 1:1000) were applied, and the slices were incubated for 2 h at room temperature. Again, after the slices were washed three times for 20 minutes each, the slices were transferred onto object slides and covered with fluorescence mounting medium (Dako, Santa Clara, USA), and a coverslip was placed on top.

Analysis of the OHSC staining

All OHSC staining experiments were analyzed using confocal laser scanning microscopy with a LSM 510 META Laser Scanning Microscope (Carl Zeiss, Jena, Germany). Light was collected through a Plan-Neofluor 10×/0.3 objective to obtain overview pictures of the hippocampal slices or a 63×/1.4 Oil DIC objective for single-cell analysis. 3D single-cell reconstructions were performed using *z*-stacks with 0.4 μm image intervals. For the Alexa Fluor 488 antibody, CaspACE FITC-VAD-FMK and ThioT staining, the fluorescence was excited at 488 nm, and emissions were detected between 505 and 550 nm. For the Alexa Fluor 546 antibody and PI staining, fluorescence was excited at 543 nm, and emissions were detected using a 560 nm long pass filter. For the Alexa Fluor 647 antibody, fluorescence was excited at 488 nm, and emissions were detected between 680 and 800 nm.

Western blot analysis

Protein concentrations were determined using a Pierce BCA Protein Assay kit (Thermo scientific, Rockford, USA) according to the manufacturer's protocol. XCell Sure Lock Mini-Cell Electrophoresis System was used to separate the proteins (Invitrogen, Karlsruhe, Germany). Protein samples were mixed with NuPAGE® LDS Sample Buffer (4×) (Life technologies, Carlsbad, USA) supplemented with 0.05 M dithiotreitol (Sigma-Aldrich, Taufkirchen, Germany) and then loaded into 10 1.5-mm NuPAGENovex 4%–12% Bis-Tris Protein Gels wells together with SeeBlue Plus2 Prestained Protein Standard (both Life technologies, Carlsbad, USA). Blots were then transferred onto nitrocellulose membranes (Whatman, Maidstone, UK) using an XCell II Blot Module (Invitrogen, Karlsruhe, Germany), and the membranes were reversibly stained using a MemCode Reversible Protein Stain Kit (Perbio Science, Bonn, Germany) to visualize that the protein had transferred. After blocking the membranes against nonspecific binding, they were incubated with primary antibodies (anti-Caspase-12, Cell Signaling, Danvers, USA; anti-GRP78, Santa Cruz, Dallas, USA; anti-Tubulin, Sigma-Aldrich, Taufkirchen, Germany; or anti-Vinculin, Sigma-Aldrich, Taufkirchen, Germany) overnight and then with peroxidase-conjugated secondary antibodies (anti-mouse peroxidase-conjugated; anti-rabbit peroxidase-conjugated; or anti-goat

peroxidase-conjugated, Vector Laboratories, Peterborough, UK) for 1 hour. To visualize bands, the membranes were incubated with SuperSignal West Dura Extended Duration Substrate (Thermo Scientific, Rockford, USA) and exposed to an autoradiographic film (CL-Xposure Film, Thermo Scientific, Rockford, USA). Films were scanned using a GS-800 Calibrated Densitometer, and densitometric analysis was performed using Quantity One software (both Bio-Rad Laboratories, Munich, Germany). Quantification was carried out by calculating the fold increase of treatment conditions in comparison to the control condition.

Cytokine ELISA for IL-6 and TNF-α

For the IL-6 and TNF-α ELISAs, mouse IL-6 ELISA Ready-SET-Go! and mouse TNF-α ELISA Ready-SET-go! kits (both eBioscience, San Diego, USA), respectively, were used according to the manufacturer's protocol. Briefly, the supernatant was collected from each OHSC during every media change (3 times), and these samples were combined before use. ELISA 96-well plates (Microlon, Greiner, Frickenhausen, Germany) were incubated overnight at 4°C with capture antibody solution in 1× coating buffer. The plate was washed with 1× PBS supplemented with 0.05% tween 20, blocked with 1× assay diluent for 1 h and then washed again. Afterward, cytokine standards and samples were applied and they were incubated for 2 h. After the plates were washed, they were incubated with a detection antibody dilution in 1× assay diluent for 1 h, followed by an additional washing step. Streptavidin-HRP was incubated for 30 minutes in 1× assay diluent. Before incubation of the plates in tetramethylbenzidine (TMB) substrate, they were washed 2 times. After 15 minutes, the reaction was stopped using 5% H_2SO_4 (Carl Roth, Karlsruhe, Germany). Absorbance was measured at 450 nm using a plate reader (Infinite M200, Tecan, Männedorf, Switzerland).

Griess assay

Nitric oxide (NO) production was measured using a colorimetric method based on a chemical diazotization reaction using Griess reagent. During every media change, the OHSC supernatant was collected (3 times), and they were combined prior to use. The samples and standards were transferred to a 96-well plate (Greiner, Frickenhausen, Germany) and incubated for 10 minutes with reagent I (1% (m/V) sulfanilamide, 5% (V/V) in phosphoric acid) at room temperature in the dark. Afterward, reagent II (0.1% (V/V) naphthylethylenediamine dihydrochloride) was added, and the plates were incubated for 10 minutes in the dark. Absorbance was measured using a plate reader (Infinite M200, Tecan, Männedorf, Switzerland) at 550 nm.

Preparation and cultivation of isolated microglia

Adult mice (Janvier, Le Genest-saint-Isle, France) were sacrificed via cervical dislocation. Embryonic mice (E13.5) were decapitated and brains were dissected. Microglial cells were obtained from the embryonic cortex and collected into Leibovitz L-15 medium (PAA Laboratories, Pasching, Austria). Afterward, the cells were homogenized and centrifuged at $300 \times g$ for 5 minutes; the remaining pellet was re-suspended in microglia culture medium (DMEM/F-12, Fetal Calf Serum, 100 U/mL penicillin and 100 µg/mL streptomycin and 200 mM L-glutamine, pH 7.2; all PAA Laboratories, Pasching, Austria). The cells were cultured in polyethylenimine-coated 6-well plates. The next day, half of the medium was changed. On day 7, the medium was supplemented with 5 ng/mL granulocyte–macrophage colony-stimulating factor (Roche, Basel, Switzerland), as previously described (12). On day 13, astrocytes were removed from the culture via trypsinization using 0.25% trypsin at 37°C. Microglial cells were re-suspended and re-plated onto PEI-coated 24- or 96-well plates at a density of 100 000–200 000 cells per mL. The cells obtained using this protocol were mainly microglia (>95%), as shown by CD11b flow cytometric analysis.

Real-time measurements of cell impedance

The xCELLigence Real-Time Cell Analyzer RTCA-MP system (Roche diagnostics, Rotkreuz, Switzerland) was used to detect changes in cellular impedance that resulted from changes in microglial morphology (11). To subtract the background, the impedance of the primary microglia medium was recorded prior to seeding the cells. Afterward, 15 000 primary microglial cells were seeded in 100 µL cell culture medium per well in 96-well format E plates (Roche diagnostics, Rotkreuz, Switzerland). After 24 h of incubation, the cells were treated with LPS (a positive control (11)) or Aβ$_{1-42}$. Cell index values were recorded during the whole treatment period using RTCA software 1.2 (Roche Diagnostics, Rotkreuz, Switzerland).

Statistical analysis

All data are shown as the mean ± standard deviation (SD). Multiple comparisons were performed using analysis of variance (ANOVA) followed by Scheffé's *post hoc* test. $P < 0.05$ was used as threshold *p*-value to define significance. Calculations were performed using the Winstat standard statistical software package (R. Fitch Software, Bad Krozingen, Germany).

RESULTS

Repeated treatment with oligomer-enriched preparations of Aβ$_{1-42}$ for 7 days does not induce neuronal cell death in OHSCs

OHSCs obtained from wild-type C57BL/6J mice, which maintained neuronal and microglial cells in the *in vivo* formation (Figure 1A), were used as an *in situ* model to study Aβ$_{1-42}$-induced neurotoxicity. OHSCs were challenged with increasing concentrations of oligomer-enriched Aβ$_{1-42}$ preparations (300–1600 nM) and were subsequently double-stained with Neuronal Nuclei (NeuN) antibody and PI (Figure 1B). Neuronal survival in the dentate gyrus (DG) and cornu ammonis (CA1+3) regions was not significantly affected in OHSCs following treatment with Aβ$_{1-42}$ for up to one week (Figure 1E).

Depletion of microglial cells enables Aβ$_{1-42}$-induced neuronal death in OHSCs

The induction of apoptosis by the use of the macrophage toxin clodronate is a well-established method for depleting microglial cells both *in vitro* (56) and *in vivo* (15). Treatment of OHSCs with clodronate has been shown to selectively deplete microglial cells without affecting other cell types (45). Clodronate (0.1 mg/mL) was applied to freshly obtained OHSCs for 24 h, resulting in OHSCs without Iba1-positive microglial cells and unaffected neuronal formations (Figure 1C). To
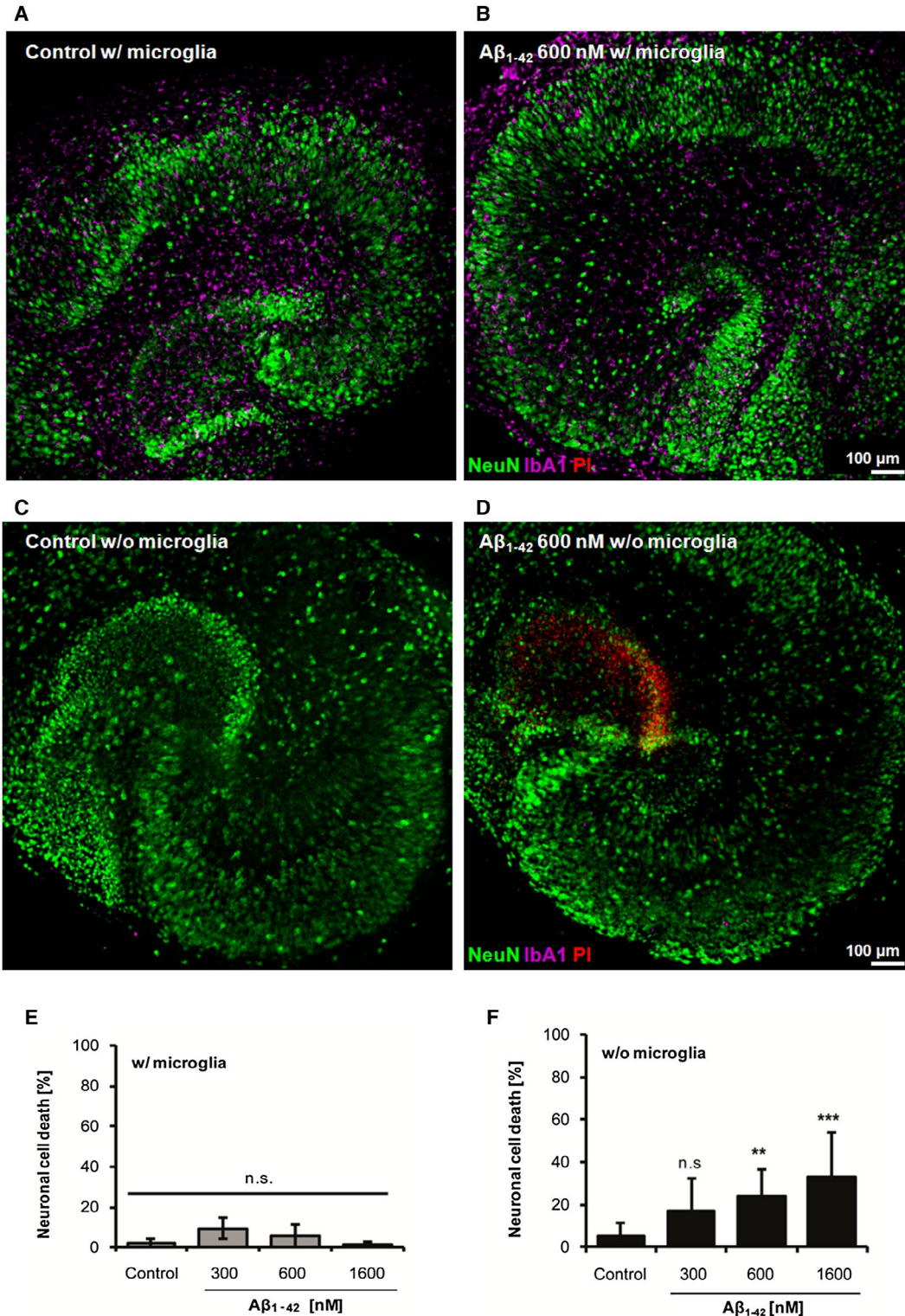
Figure 1. *Selective depletion of microglial cells by clodronate facilitates Aβ$_{1-42}$-induced neurotoxicity in OHSCs.* **A.** Representative image of an untreated OHSC stained with PI (dead cells), NeuN (neurons) and Iba1 (microglia) after 13 days in culture. **B.** Representative image of an OHSC after 7 days of repeated treatment with 600 nM Aβ$_{1-42}$. The OHSC was stained with PI, NeuN and Iba1. **C.** Representative image of an untreated OHSC depleted of microglia by treatment with clodronate (100 μg/mL, 24 h) and then stained with PI (dead cells), NeuN (neurons) and Iba1 (microglia) after 13 days in culture. **D.** Representative image of a microglia-depleted OHSC after 7 days of repeated treatment with 600 nM Aβ$_{1-42}$. The OHSC was stained with PI, NeuN and Iba1. **E.** Quantification of neuronal cell death after 7 days of treatment with different concentrations Aβ$_{1-42}$. OHSCs were stained with PI and NeuN, and the amount of dead neurons [%] was calculated as the red area (PI) divided by the green area (NeuN) in the hippocampal regions CA1+3 and DG (mean ± SD; 11–19 individual slices per condition from 3 independent preparations, n.s. *P* > 0.05). **F.** Quantification of neuronal cell death after 7 days of treatment with different concentrations of Aβ$_{1-42}$ in OHSCs depleted of microglia. OHSCs were stained with PI, NeuN and Iba1. Only slices in which less than 10% of the hippocampal regions CA1+3 and DG were covered by Iba1-positive microglia were used for quantification. The amount of dead neurons [%] was calculated as the red area (PI) divided by the green area (NeuN) in the hippocampal regions CA1+3 and DG (mean ± SD; 7–15 individual slices per condition from 3 independent preparations, n.s. *P* > 0.05, **P < 0.01, ***P < 0.001 compared to the untreated control).

investigate the role of microglia in Aβ$_{1-42}$-induced effects, microglia-depleted OHSCs were incubated with increasing concentrations of oligomer-enriched preparations of Aβ$_{1-42}$ (300–1600 nM) and then analyzed to determine whether there were changes in neuronal cell death (Figure 1D). Concentrations starting from 600 nM Aβ$_{1-42}$ significantly increased neuronal cell death in OHSCs that had been depleted of microglia compared to untreated control OHSCs (Figure 1F).

Microglial cells prevent ER stress and caspase cleavage in Aβ$_{1-42}$-challenged OHSCs

Aβ$_{1-42}$ oligomers induced neuronal apoptosis via caspase-dependent pathways (2, 70). To investigate neuronal caspase activity in OHSCs, we applied a fluorescent analog of the pan-caspase inhibitor Z-VAD-FMK, which allows for detection of activated caspases, over a time period of 48 h and then performed counterstainings for NeuN. We did not detect a significant increase in neuronal caspase cleavage after Aβ$_{1-42}$ treatment within 48 h. However, the depletion of microglial cells strongly enhanced the expression of activated caspases after the challenge with Aβ$_{1-42}$ (Figure 2A,B). In addition, previous studies have indicated that treatment with Aβ potentiates ER stress-induced expression of caspase-12 in OHSCs (43). According to recent investigations, Aβ oligomers are able to move between the intracellular and the extracellular space (22, 82) and may mediate toxicity on both levels. Interestingly, Aβ oligomers were detected in the ER of hippocampal neurons in a mouse model of AD where they are supposed to induce organelle functional impairment resulting ultimately in cell death (86). Furthermore, recent evidence suggests that Aβ oligomers induce defects in lipid bilayers, thus, inducing rapid calcium influx (48) which may affect the ER as the main intracellular calcium store. Therefore, we next aimed to investigate whether Aβ-mediated toxicity in microglia-depleted OHSC may be accompanied by upregulation of ER stress marker proteins. We found that cleavage of caspase-12 occurred only in OHSCs that had been depleted of microglial cells and was enhanced by Aβ$_{1-42}$ treatment, as shown by Western Blot analysis (Figure 2C). We next investigated a second ER stress marker, the ER resident chaperone GRP78. GRP78 protein expression was not affected by either microglial cell depletion or treatment alone. However, Aβ$_{1-42}$ treatment in microglia-depleted OHSCs resulted in enhanced GRP78

expression (Figure 2D), suggesting that microglial cells inhibited Aβ$_{1-42}$-induced ER stress.

Microglial cells provide their protective effect in a ramified morphological state

Under physiological conditions, microglial cells display a ramified morphology that has long been defined as their "resting phenotype." Nevertheless, recent data indicate that ramified microglia are not "resting" but are actively scanning their environment to maintain tissue homeostasis (21, 30, 50).

We treated OHSCs with Aβ$_{1-42}$ for 7 days and then investigated the morphology of microglia using Iba1 staining. LPS treatment for 24 h, which was used as a positive control to induce full microglial pro-inflammatory activation, is characterized by a morphological transition toward amoeboid cells. It is described here that Aβ$_{1-42}$ treatment did not change the morphological properties of microglia compared to microglia from untreated OHSCs (Figure 3A). For an additional quantitative assessment of microglial responses, we used real-time impedance measurements of pure microglia cultures. These measurements provide information related to changes in microglial morphology, which were continuously monitored for the entire Aβ$_{1-42}$ challenge period. LPS induced marked alterations in microglial structural features, as detected using xCELLigence measurements. Treatment with high concentrations (20 μM) of oligomer-enriched Aβ$_{1-42}$ preparations, however, did not induce changes in microglial morphology, as measured using an xCELLigence system (Figure 3B).

In addition to morphological changes, the pro-inflammatory activation of microglia resulted in the increased production of pro-inflammatory cytokines and NO release. Therefore, levels of pro-inflammatory cytokines were examined after 7 days of Aβ$_{1-42}$ treatment. LPS treatment for 24 h was used as a positive control. In OHSCs in which microglial cells were present, Aβ$_{1-42}$ treatment alone did not significantly increase IL-6 (Figure 4A), TNF-α (Figure 4B) or NO levels (Figure 4C). According to these data, Aβ$_{1-42}$ treatment did not result in microglia with a pro-inflammatory phenotype. Therefore, a morphological transition or pro-inflammatory activity of ramified microglia seemed to be unnecessary for improving neuronal survival after Aβ$_{1-42}$ treatment in OHSCs.
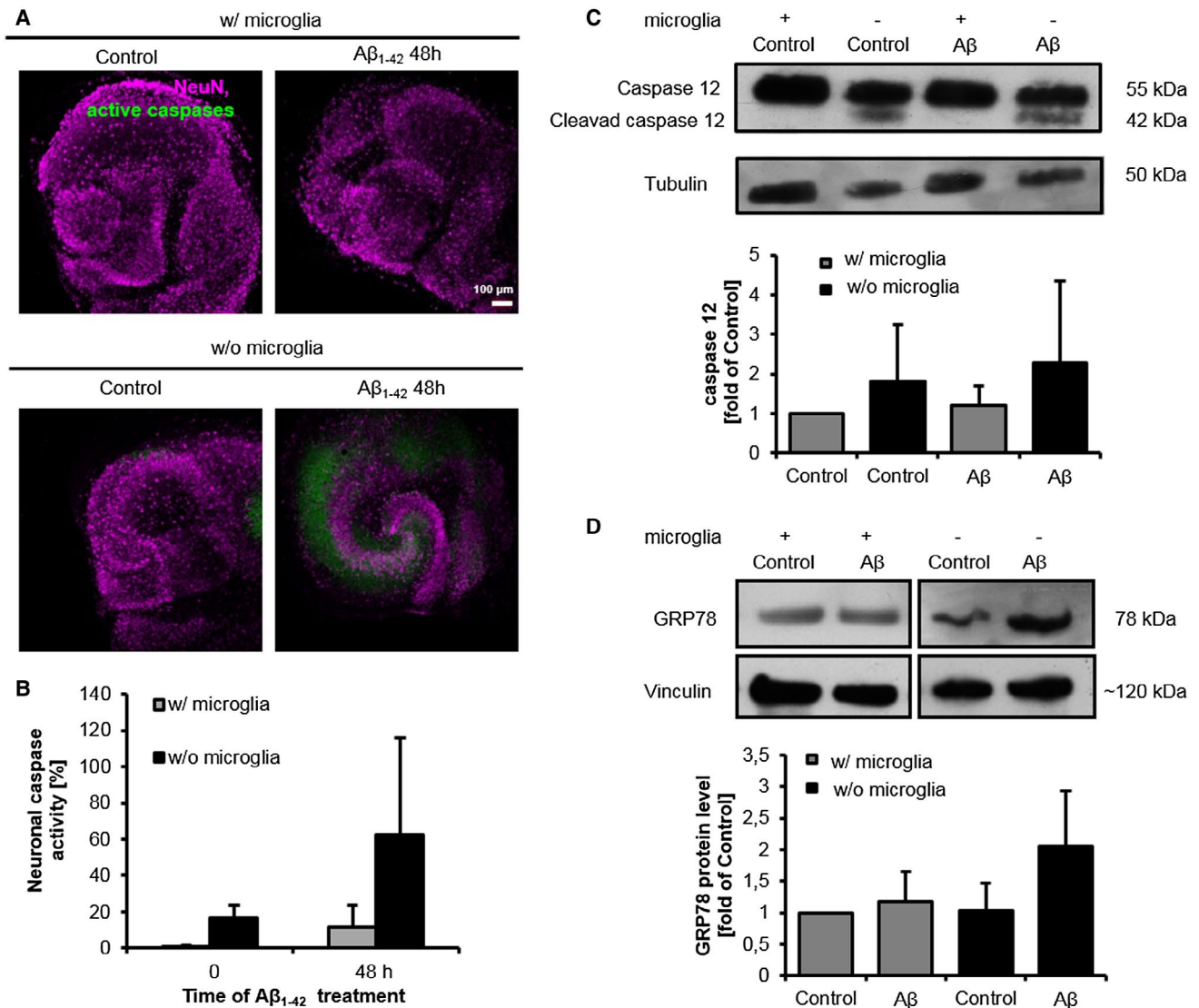
Figure 2. *Aβ$_{1-42}$ treatment in OHSCs results in ER stress and caspase cleavage only in the absence of microglial cells.* **A.** Representative images from different treatment conditions after CaspACE™ FITC-VAD-FMK staining for activated caspases and NeuN immunostaining for neurons. **B.** Quantification of neuronal caspase activity in OHSCs after 48 h of treatment with 600 nM Aβ$_{1-42}$. The caspase staining within one hippocampal slice was calculated as the green area (CaspACE FITC-VAD-FMK positive) divided by the far-red area (NeuN) (mean ± SD; 8–17 individual slices per condition from 3 independent preparations,

***$P < 0.001$ compared to treatment for 48 h with Aβ$_{1-42}$ with microglial cells present). **C.** Representative Western blot for caspase-12 and cleaved caspase-12 after 48 h of treatment with 600 nM Aβ$_{1-42}$ with and without microglial cells present. Corresponding densitometric quantification is shown (mean ± SD; n = 3). D) Representative Western blot for GRP78 after 48 h of treatment with 600 nM Aβ$_{1-42}$ with and without microglial cells present. Corresponding densitometric quantification is shown (mean ± SD; n = 3).

Phagocytosis of Aβ$_{1-42}$ contributes to the neuroprotective effects of microglia

Previous *in vitro* studies revealed the ability of microglia to take up Aβ (18, 20, 29, 64). However, it is unknown whether microglial uptake of Aβ reduces peptide toxicity to contribute to neuronal survival. Here, we performed Thioflavin T (ThioT) staining to investigate whether the increase in neuronal death observed after Aβ$_{1-42}$ treatment in microglia-free OHSCs was accompanied by an enhanced Aβ plaque load. First, we

confirmed that microglial cells were able to engulf ThioT-positive Aβ$_{1-42}$ in OHSCs using *z*-stack analysis of ThioT and Iba1 expression in single microglial cells (Figure 5A). Next, we compared ThioT staining in OHSCs with and without microglial cells (Figure 5B,C). The analysis of ThioT-positive areas of microglia-depleted OHSCs following Aβ$_{1-42}$ treatment for 48 h did not result in a significant difference compared to non-treated OHSCs (Figure 5C). In contrast, significant increases in hippocampal areas positive for ThioT were observed
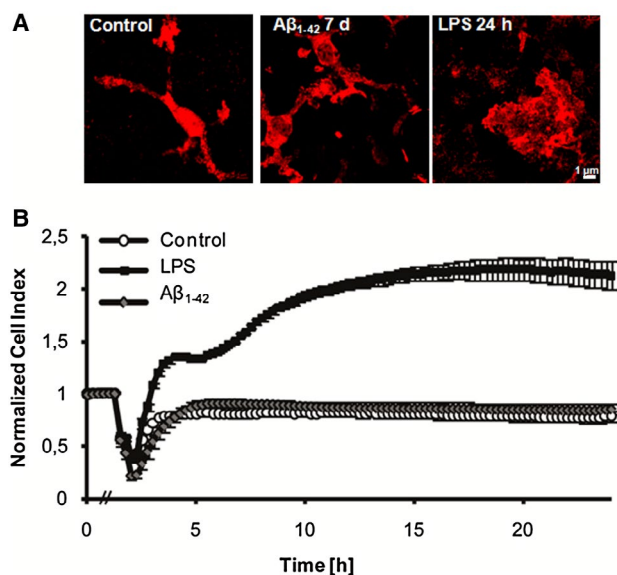
Figure 3. *Microglial morphology after Aβ$_{1-42}$ treatment.* **A.** Microglial morphology was assessed using Iba1 staining in untreated OHSCs and after 24 h of treatment with LPS 1 µg/mL or 7 days of treatment with Aβ$_{1-42}$ 600 nM. **B.** Real-time detection of morphological changes in untreated pure microglial cultures and after treatment with 1 µg/mL LPS or 20 µM Aβ$_{1-42}$. Values were normalized to 1 before treatment (mean ± SD; n = 6).

after 7 days of treatment with Aβ$_{1-42}$ in microglia-free slices, indicating that Aβ plaques formed in this *ex vivo* model.

To further investigate the impact of microglial Aβ$_{1-42}$ uptake on neuronal survival in OHSCs, we applied cytochalasin D, a blocker of actin polymerization that inhibits the phagocytic activity of microglia (64, 74) at a concentration that was barely neurotoxic in OHSC (52). Treatment with cytochalasin D resulted in a significant increase in the hippocampal area that was positive for ThioT, suggesting efficient inhibition of microglial Aβ$_{1-42}$ intake (Figure 5D). Inhibiting microglial uptake mechanisms with cytochalasin D increased the number of dead neurons that were positive for PI staining following treatment with Aβ$_{1-42}$ (Figure 5E), indicating that Aβ$_{1-42}$ phagocytosis contributes to microglia-mediated protective effects.

DISCUSSION

Our study provides evidence that the presence of ramified microglia reduces Aβ$_{1-42}$-mediated neurotoxicity in postnatal wild-type OHSCs. This reduction in neuronal cell death was accompanied by a reduced Aβ load, suggesting an important neuroprotective role for microglial phagocytosis.

OHSC as a model to investigate neuron–glia interactions

To characterize and understand the roles of microglia in AD pathology, it is essential to use appropriate models. For many years, pure, isolated microglial cultures were used
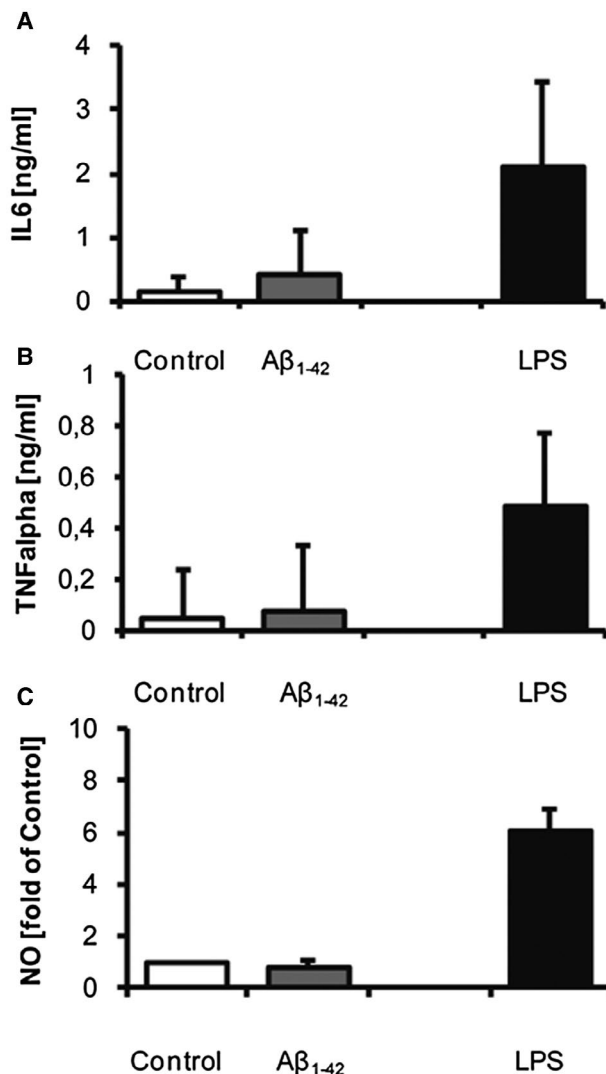

Figure 4. *Microglial release of pro-inflammatory mediators after Aβ$_{1-42}$ treatment.* **A-C.** The release of pro-inflammatory mediators was investigated in OHSC supernatants using ELISA measurements of TNF-α and IL-6 levels and Griess assays for NO release. OHSCs were treated with 100 µg/mL LPS for 24 h or 600 nM Aβ$_{1-42}$ for 7 days (mean ± SD, data pooled from at least 4 independent experiments).

for investigation. However, one of the great disadvantages of the use of isolated microglial cultures is the lack of inhibitory signals that arise from neurons (7, 32, 37). Accordingly, several expression studies have provided evidence that standard cultured microglia are more similar to peripheral myeloid cells than to *in vivo* microglia (4, 6). This may explain why most of the studies that investigated the influence of isolated microglia on neuronal survival described the neurotoxic potential of these cells (5, 24, 47), which is in contrast to our current findings. In the present study, OHSCs were used as a model system to investigate the interplay between microglia and neurons in a pathology relevant to AD. Because microglia in OHSCs maintain their *in vivo* environment and exhibit a ramified morphology

(78, 88) that is comparable to their appearance *in vivo* (64), the use of OHSCs is thought to be more appropriate for disease modeling than cultures containing single-cell types. The reagent bisphosphonate clodronate has long been used to deplete microglial cells *in vitro* as well as *in vivo* (15, 56), and it has never affected the number and integrity of neurons in these different studies. Hence, the depletion of microglial cells from OHSCs using clodronate serves as an
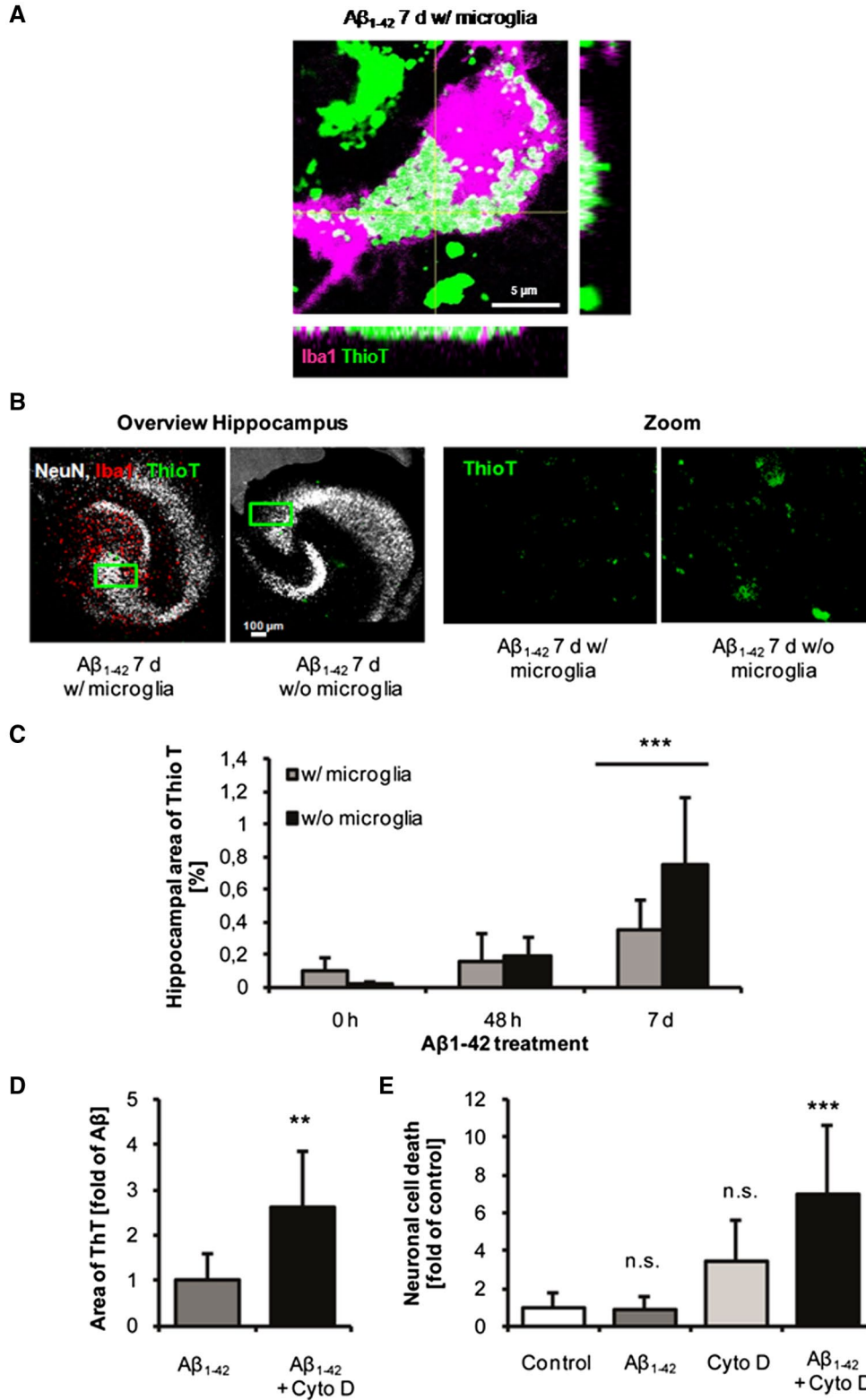
© 2019 The Authors. Brain Pathology published by John Wiley & Sons Ltd on behalf of International Society of Neuropathology

Figure 5. *Phagocytosis of Aβ$_{1-42}$ contributes to the neuroprotective effects of microglia.* **A.** A 3-D image was created using *z*-stacks showing ThioT and Iba1 staining in a single microglial cell from an OHSC that was treated with 600 nM Aβ$_{1-42}$ for 7 days. Cross indicates sagittal and transversal section planes. **B.** Representative images showing ThioT, NeuN and Iba1 staining in OHSCs after 7 days of repeated treatment with 600 nM Aβ$_{1-42}$ with (1) and without (2) microglial cells present; a fivefold magnification of ThioT staining is given. **C.** Quantification of ThioT-positive hippocampal areas after treatment with 600 nM Aβ$_{1-42}$ for the indicated times (mean ± SD; 12–18 individual slices per condition from 3 independent preparations, ***P < 0.001 compared to 7 days of

Aβ$_{1-42}$ treatment in the presence of microglia). **D.** Assessment of ThioT staining after treatment with Aβ$_{1-42}$ in the presence and absence of the phagocytosis blocker Cytochalasin D (mean ± SD; 8–13 individual slices per condition, **P < 0.01 compared to treatment with Aβ$_{1-42}$). **E.** Quantification of neuronal cell death after 7 days of treatment with Aβ$_{1-42}$ and Cytochalasin D. OHSCs were stained with PI and NeuN, and the amount of dead neurons [%] was calculated as the red area (PI) divided by the green area (NeuN) in the hippocampal regions CA1+3 and DG (mean ± SD; n = 7–9 per condition, ***P < 0.001 compared to the control).

excellent tool for investigating the impact of microglia on Aβ-mediated effects.

Aβ$_{1-42}$-mediated effects on neurons in OHSCs

In the present study, exogenous Aβ$_{1-42}$ peptide, in nanomolar concentrations (up to 1.6 µM), was repetitively applied to OHSCs for one week, starting on days 6–7 in culture. The Aβ$_{1-42}$ concentrations used were in the range of the concentrations described for Aβ levels in AD patients' brains (71). Nevertheless, treatment with Aβ$_{1-42}$ oligomer-enriched preparations did not result in neuronal cell death in OHSCs, as shown by the results of PI staining (Figure 1). This is in line with previous studies that showed that applying different Aβ species (Aβ$_{1-28}$, Aβ$_{25-35}$, Aβ$_{1-40}$) for various durations (24 h–7 d) failed to trigger neuronal cell death in OHSCs (63, 87, 90). In contrast, numerous studies have described the neurotoxic potential of oligomer-enriched Aβ preparations in OHSCs. However, in most of these studies, OHSCs were treated in serum-free (55, 80, 89) or serum-reduced (41, 54) media, or the Aβ treatment was combined with other detrimental stimuli (3, 43) to boost toxicity. In addition, higher concentrations, ranging from 2 to 10 µM Aβ$_{1-42}$, resulted in significant neuronal cell death in OHSCs after 24–48 h of treatment (42, 51, 93). The concentrations used in these experiments are, however, thought to be far from those observed under physiological settings in AD.

Previous studies have shown that Aβ-mediated cell death is caspase-dependent in pure neuronal cultures (2, 70). Regarding OHSCs, treatment with Aβ$_{25-35}$ and Aβ$_{1-42}$ at high micromolar concentrations resulted in the cleavage of caspase-3 (19), suggesting its involvement in Aβ-mediated apoptosis. In our experimental setting, staining for activated caspases indicated that Aβ$_{1-42}$-mediated cell death mechanisms are caspase-dependent in the absence of microglia (Figure 2A,B). Furthermore, the enhanced expression of ER stress marker proteins implies that ER stress pathways may be involved in Aβ$_{1-42}$-induced toxicity in absence of microglia (Figure 2C,D). Aβ treatment has been previously demonstrated to result in caspase-12-mediated cell death mechanisms and enhanced expression levels of GRP78 in primary neuronal cultures (70, 94). In contrast, cleavage of caspase-12 or the upregulation of GRP78 after treatment with Aβ$_{25-35}$ was not detected in OHSCs (43). In addition, treatment with Aβ for 48 h resulted in the cleavage of caspase-12 only in old OHSCs that were cultured for 7 weeks (44), suggesting that ER

stress pathways may be involved in Aβ-mediated cell death in neurons. However, the presence of functional ramified microglia may be sufficient to block this route of toxicity.

Aβ$_{1-42}$-mediated effects on microglia in OHSC

As described earlier, activated microglia are found in the surrounding of amyloid plaques indicating an interaction with amyloid oligomers and fibrils (16). Supporting evidence for an involvement of amyloid oligomers in the activation of microglial cells is derived from the fact that on microglial cells, receptors were found capable of binding to Aβ$_{1-42}$ (58, 69).

Binding to these receptors activates a signaling cascade resulting in the expression of cytokines of either pro- or anti-inflammatory origin or leads to the internalization of abeta molecules. Furthermore, when microglia face such inflammation sites for the first time, they are said to be "primed" and undergo a change in their morphology toward an amoeboid appearance (34, 60). In the present study, however, treatment of OHSCs with Aβ$_{1-42}$ oligomer-enriched preparations for 7 days did not result in the classical signs of microglial activation, including significant increases in the release of the pro-inflammatory cytokines IL-6 and TNF-α and NO secretion (Figure 4) and a switch in morphology toward an amoeboid phenotype (Figure 3). Besides, the above described activation states, Wyss-Coray and Rogers summarized in 2012, another phenotype which is "acquired deactivation" (9, 26, 92). The term was first introduced by Gordon in 2003 and differs from the "classical alternative activation state," also formerly known as M2, in the way, that next to cytokines (Interleukins (IL-10); Tumor growth factor-β (TGF-β)) also apoptotic cells themselves can give rise to this second alternative state (9, 25, 68). Microglial cells with this phenotype are said to be "immunosuppressive" and are not capable of producing cytokines of either pro- or anti-inflammatory origin. Besides, their main function is to take up apoptotic cells. The reason we did not observe an amoeboid phenotype in our experimental setup could be that the microglial cells were not activated classically by amyloid oligomeric structures, but still "active" in the way of clearing cellular debris by maintaining a ramified phenotype.

In contrast, previous studies that used the same Aβ$_{1-42}$ oligomer-enriched preparations but at higher micromolar concentrations (10 µM) demonstrated IL-6 and TNF-α release from primary microglial cultures (23), thereby indicating a potential difference between microglia used in suspension cultures and microglia in *ex vivo* models. However, in former

OHSCs studies, treatment with Aβ$_{1-40}$ (8) and Aβ$_{25-35}$ (41) at higher micromolar concentrations resulted in the enhanced expression of IL-6 and TNF-α, while nanomolar concentrations of Aβ$_{1-42}$ (20 nM) did not induce detectable increases in IL-6 and TNF-α release (62), suggesting that either high concentrations or different Aβ preparations (or a combination of both) are sufficient to promote the release of pro-inflammatory cytokines from microglia in OHSCs.

One previous investigation using an OHSC model demonstrated that stimulation with Aβ$_{1-42}$ oligomers results in enhanced NO release from microglia (62). The authors identified NO as the major mediator of Aβ$_{1-42}$ oligomer-induced microglial neurotoxicity. Therefore, the absence of NO in the present study may explain the lack of neurotoxicity induced by the Aβ$_{1-42}$ oligomer preparation we used. Nevertheless, it remains unknown why these two different studies reached such different results. Differences in the Aβ oligomerization protocols used may partly explain this phenomenon. In the former study by Maezawa and colleagues, however, NO-mediated microglial neurotoxicity was accompanied by the presence of an amoeboid phenotype (62), indicating that this kind of morphologically activated microglia can also promote the death of neurons.

Ramified microglia provide protection against Aβ$_{1-42}$ toxicity

In the present study, the presence of ramified microglia prevented Aβ$_{1-42}$-mediated neuronal cell death, while the depletion of microglial cells facilitated neuronal tissue damage, suggesting a protective effect by microglia.

OHSCs were obtained from postnatal, healthy, wild-type mice, microglia were uniformly distributed throughout the hippocampal slices used in the cultures (Figure 1A), and they exhibited a ramified morphology (Figure 3A), suggesting that the functional integrity of the microglia was preserved in the experimental setting. Interestingly, treatment of the slices with Aβ$_{1-42}$ for 7 d did not affect their ramified morphological state (Figure 3A).

The neuroprotective properties of non-ramified microglial cells are well described in OHSC models of excitotoxicity (85) or stroke *in vivo* (15, 57) and to a lesser extent for ramified microglia (65, 88). Furthermore, a few studies have been performed to investigate the role of microglial cells in *in vivo* and *ex vivo* models of neurodegenerative diseases. In OHSCs obtained from CD11b-HSVTK mice, inducing the removal of microglial cells with ganciclovir increased prion titers 15-fold, suggesting a beneficial role for microglia in prion infections (13). However, in a mouse model of ALS in which the mice carried a superoxide dismutase (SOD) mutation, depleting microglial cells did not affect disease progression (27), whereas *in vivo* microglial depletion from wild-type CB57BL/6 mice was shown to worsen brain ischemia and to enhance neuroinflammation by upregulating important pro-inflammatory cytokines as well as increased neuronal cell death (46, 81). Regarding transgenic mouse models of AD, depleting microglial cells did not affect Aβ plaque load *in vivo* (28). However, as the here presented data and recent findings suggest that microglia prevent the formation of Aβ plaques (33), this lack of effect on Aβ plaque load in AD models might be due to rather late time point were microglia have been depleted. It is moreover important to note that severe neurodegeneration, like that observed in AD patients, does not take place in the used transgenic animals (28), which makes it difficult to address the impact of microglia on AD-related neurodegeneration in these models *in vivo*. Therefore, clodronate-induced microglial depletion in OHSCs is an excellent tool for addressing this particular point. To the best of our knowledge, the present study is the first to demonstrate a beneficial effect for ramified microglia in Aβ-mediated neurotoxicity in an *ex vivo* model of AD.

Several mechanisms were described that may contribute to the microglia-mediated neuroprotective effects observed in models of Aβ$_{1-42}$-mediated toxicity. These include the release of neurotrophic factors that may provide trophic support to surrounding neurons and neuronal processes (21) in addition to the ability to take up toxic substances, such as glutamate, from the extracellular environment and to render them harmless (30). Here, depleting microglial cells increased the Aβ load and resulted in neuronal apoptosis. Furthermore, efficiently blocking microglial uptake mechanisms with cytochalasin D resulted in a significant increase in neuronal cell death in OHSCs that were challenged with Aβ$_{1-42}$ oligomer-enriched preparations (Figure 5E). We thus confirmed and elaborated recent findings that microglia in OHSCs take up Aβ (33, 91), which corroborates *in vivo* studies demonstrating that microglia from wild-type mice efficiently engulf Aβ (53, 83). By reducing the Aβ load in the brain, microglia are thought to contribute to neuroprotection against AD pathology (21, 30, 31). Nevertheless, only a few studies have experimentally demonstrated the effects of microglial Aβ phagocytosis on neuronal damage (66, 84). By investigating Aβ plaque load and neuronal cell death following the depletion of microglial cells and by using microglial uptake blockers, the present study provides evidence showing that microglial Aβ engulfment is involved in the beneficial effects of microglia in OHSCs.

Our study demonstrates a potential protective role for functional ramified microglia against Aβ-mediated apoptotic mechanisms, most likely via clearance of Aβ deposits.

CONFLICT OF INTEREST

The authors declare no conflict of interest concerning the content of the article.

DATA AVAILABILITY STATEMENT

The authors confirm that all data underlying the findings are fully available without restriction. All relevant data are within the paper.

REFERENCES

1. Aguzzi A, Barres BA, Bennett ML (2013) Microglia: scapegoat, saboteur, or something else? *Science (New York, N.Y.)* **339**:156–161.

2. Alberdi E, Sánchez-Gómez MV, Cavaliere F, Pérez-Samartín A, Zugaza JL, Trullas R *et al* (2010) Amyloid beta oligomers induce Ca²⁺ dysregulation and neuronal death through activation of ionotropic glutamate receptors. *Cell Calcium* **47**:264–272.

3. Bai J-Z, Lipski J (2014) Involvement of TRPV4 channels in Aβ(40)-induced hippocampal cell death and astrocytic Ca(2+) signalling. *Neurotoxicology* **41**:64–72.

4. Beutner C, Linnartz-Gerlach B, Schmidt SV, Beyer M, Mallmann MR, Staratschek-Jox A *et al* (2013) Unique transcriptome signature of mouse microglia. *Glia* **61**:1429–1442.

5. Burguillos MA, Deierborg T, Kavanagh E, Persson A, Hajji N, Garcia-Quintanilla A *et al* (2011) Caspase signalling controls microglia activation and neurotoxicity. *Nature* **472**:319–324.

6. Butovsky O, Jedrychowski MP, Moore CS, Cialic R, Lanser AJ, Gabriely G *et al* (2014) Identification of a unique TGF-β-dependent molecular and functional signature in microglia. *Nat Neurosci* **17**:131–143.

7. Cardona AE, Pioro EP, Sasse ME, Kostenko V, Cardona SM, Dijkstra IM *et al* (2006) Control of microglial neurotoxicity by the fractalkine receptor. *Nat Neurosci* **9**:917–924.

8. Clapp-Lilly KL, Smith MA, Perry G, Duffy LK (2001) Melatonin reduces interleukin secretion in amyloid-beta stressed mouse brain slices. *Chem Biol Interact* **134**:101–107.

9. Colton CA (2009) Heterogeneity of microglial activation in the innate immune response in the brain. *J Neuroimmune Pharmacol* **4**:399–418.

10. Cornejo VH, Hetz C (2013) The unfolded protein response in Alzheimer's disease. *Semin Immunopathol* **35**:277–292.

11. Dolga AM, Letsche T, Gold M, Doti N, Bacher M, Chiamvimonvat N *et al* (2012) Activation of KCNN3/SK3/K(Ca)2.3 channels attenuates enhanced calcium influx and inflammatory cytokine production in activated microglia. *Glia* **60**:2050–2064.

12. Esen N, Kielian T (2007) Effects of low dose GM-CSF on microglial inflammatory profiles to diverse pathogen-associated molecular patterns (PAMPs). *Journal of Neuroinflammation* **4**:10.

13. Falsig J, Julius C, Margalith I, Schwarz P, Heppner FL, Aguzzi A (2008) A versatile prion replication assay in organotypic brain slices. *Nat Neurosci* **11**:109–117.

14. Farfara D, Lifshitz V, Frenkel D (2008) Neuroprotective and neurotoxic properties of glial cells in the pathogenesis of Alzheimer's disease. *J Cell Mol Med* **12**:762–780.

15. Faustino JV, Wang X, Johnson CE, Klibanov A, Derugin N, Wendland MF *et al* (2011) Microglial cells contribute to endogenous brain defenses after acute neonatal focal stroke. *J Neurosci* **31**:12992–13001.

16. Ferretti MT, Bruno MA, Ducatenzeiler A, Klein WL, Cuello AC (2012) Intracellular Abeta-oligomers and early inflammation in a model of Alzheimer's disease. *Neurobiol Aging* **33**:1329–1342.

17. Fetler L, Amigorena S (2005) Neuroscience. Brain under surveillance: the microglia patrol. *Science (New York, N.Y.)* **309**:392–393.

18. Fleisher-Berkovich S, Filipovich-Rimon T, Ben-Shmuel S, Hülsmann C, Kummer MP, Heneka MT (2010) Distinct modulation of microglial amyloid β phagocytosis and migration by neuropeptides (i). *J Neuroinflammation* **7**:61.

19. Frozza RL, Horn AP, Hoppe JB, Simao F, Gerhardt D, Comiran RA *et al* (2009) A comparative study of beta-amyloid peptides Abeta1-42 and Abeta25-35 toxicity in organotypic hippocampal slice cultures. *Neurochem Res* **34**:295–303.

20. Fu H, Liu B, Frost JL, Hong S, Jin M, Ostaszewski B *et al* (2012) Complement component C3 and complement receptor type 3 contribute to the phagocytosis and clearance of fibrillar Aβ by microglia. *Glia* **60**:993–1003.

21. Garden GA, Moller T (2006) Microglia biology in health and disease. *J Neuroimmune Pharmacol* **1**:127–137.

22. Gaspar RC, Villarreal SA, Bowles N, Hepler RW, Joyce JG, Shughrue PJ (2010) Oligomers of beta-amyloid are sequestered into and seed new plaques in the brains of an AD mouse model. *Exp Neurol* **223**:394–400.

23. Gold M, Dolga AM, Koepke J, Mengel D, Culmsee C, Dodel R *et al* (2014) α1-antitrypsin modulates microglial-mediated neuroinflammation and protects microglial cells from amyloid-β-induced toxicity. *J Neuroinflammation* **11**:165.

24. Golde S, Coles A, Lindquist JA, Compston A (2003) Decreased iNOS synthesis mediates dexamethasone-induced protection of neurons from inflammatory injury in vitro. *Eur J Neuorsci* **18**:2527–2537.

25. Gordon S (2003) Alternative activation of macrophages. *Nat Rev Immunol* **3**:23–35.

26. Gordon S, Taylor PR (2005) Monocyte and macrophage heterogeneity. *Nat Rev Immunol* **5**:953–964.

27. Gowing G, Philips T, van Wijmeersch B, Audet J-N, Dewil M, van den Bosch L *et al* (2008) Ablation of proliferating microglia does not affect motor neuron degeneration in amyotrophic lateral sclerosis caused by mutant superoxide dismutase. *J Neurosci* **28**:10234–10244.

28. Grathwohl SA, Kalin RE, Bolmont T, Prokop S, Winkelmann G, Kaeser SA *et al* (2009) Formation and maintenance of Alzheimer's disease beta-amyloid plaques in the absence of microglia. *Nat Neurosci* **12**:1361–1363.

29. Griciuc A, Serrano-Pozo A, Parrado AR, Lesinski AN, Asselin CN, Mullin K *et al* (2013) Alzheimer's disease risk gene CD33 inhibits microglial uptake of amyloid beta. *Neuron* **78**:631–643.

30. Hanisch U-K, Kettenmann H (2007) Microglia: active sensor and versatile effector cells in the normal and pathologic brain. *Nat Neurosci* **10**:1387–1394.

31. Hansen DV, Hanson JE, Sheng M (2018) Microglia in Alzheimer's disease. *J Cell Biol* **217**:459–472.

32. Hellwig S, Heinrich A, Biber K (2013) The brain's best friend: microglial neurotoxicity revisited. *Front Cell Neurosci* **7**:71.

33. Hellwig S, Masuch A, Nestel S, Katzmarski N, Meyer-Luehmann M, Biber K (2015) Forebrain microglia from wild-type but not adult 5xFAD mice prevent amyloid-β plaque formation in organotypic hippocampal slice cultures. *Sci Rep* **5**:14624.

34. Heneka MT, Carson MJ, Khoury JE, Landreth GE, Brosseron F, Feinstein DL *et al* (2015) Neuroinflammation in Alzheimer's disease. *Lancet Neurol* **14**:388–405.

35. Heneka MT, Kummer MP, Latz E (2014) Innate immune activation in neurodegenerative disease. *Nat Rev Immunol* **14**:463–477.

36. Heppner FL, Ransohoff RM, Becher B (2015) Immune attack: the role of inflammation in Alzheimer disease. *Nat Rev Neurosci* **16**:358–372.

37. Hoek RM, Ruuls SR, Murphy CA, Wright GJ, Goddard R, Zurawski SM *et al* (2000) Down-regulation of the macrophage lineage through interaction with OX2 (CD200). *Science (New York, N.Y.)* **290**:1768–1771.

38. Holopainen IE (2005) Organotypic hippocampal slice cultures: a model system to study basic cellular and molecular mechanisms of neuronal cell death, neuroprotection, and synaptic plasticity. *Neurochem Res* **30**:1521–1528.

39. Hoozemans JJM, van Haastert ES, Nijholt DAT, Rozemuller AJM, Eikelenboom P, Scheper W (2009) The unfolded protein response is activated in pretangle neurons in Alzheimer's disease hippocampus. *Am J Pathol* **174**:1241–1251.

40. Hoozemans JJM, Veerhuis R, van Haastert ES, Rozemuller JM, Baas F, Eikelenboom P *et al* (2005) The unfolded protein response is activated in Alzheimer's disease. *Acta Neuropathol* **110**:165–172.

41. Hoppe JB, Frozza RL, Horn AP, Comiran RA, Bernardi A, Campos MM *et al* (2010) Amyloid-beta neurotoxicity in organotypic culture is attenuated by melatonin: involvement of GSK-3beta, tau and neuroinflammation. *J Pineal Res* **48**:230–238.

42. Hoppe JB, Haag M, Whalley BJ, Salbego CG, Cimarosti H (2013) Curcumin protects organotypic hippocampal slice cultures from Aβ1-42-induced synaptic toxicity. *Toxicol In Vitro* **27**:2325–2330.

43. Imai T, Kosuge Y, Ishige K, Ito Y (2007) Amyloid beta-protein potentiates tunicamycin-induced neuronal death in organotypic hippocampal slice cultures. *Neuroscience* **147**:639–651.

44. Ishige K, Takagi N, Imai T, Rausch WD, Kosuge Y, Kihara T *et al* (2007) Role of caspase-12 in amyloid beta-peptide-induced toxicity in organotypic hippocampal slices cultured for long periods. *J Pharmacol Sci* **104**:46–55.

45. Ji K, Akgul G, Wollmuth LP, Tsirka SE (2013) Microglia actively regulate the number of functional synapses. *PLoS ONE* **8**:e56293.

46. Jin W-N, Shi SX-Y, Li Z, Li M, Wood K, Gonzales RJ *et al* (2017) Depletion of microglia exacerbates postischemic inflammation and brain injury. *J Cerebr Blood Flow Metab* **37**:2224–2236.

47. Kaushal V, Koeberle PD, Wang Y, Schlichter LC (2007) The Ca2+-activated K+ channel KCNN4/KCa3.1 contributes to microglia activation and nitric oxide-dependent neurodegeneration. *J Neurosci* **27**:234–244.

48. Kayed R, Lasagna-Reeves CA (2013) Molecular mechanisms of amyloid oligomers toxicity. *J Alzheimer's Dis* **33**(Suppl. 1):S67–S78.

49. Kettenmann H, Hanisch U, Noda M, Verkhratsky A (2011) Physiology of microglia. *Physiol Rev* **91**:461–553.

50. Kettenmann H, Hanisch U-K, Noda M, Verkhratsky A (2011) Physiology of microglia. *Physiol Rev* **91**:461–553.

51. Kim H-J, Chae S-C, Lee D-K, Chromy B, Lee SC, Park Y-C *et al* (2003) Selective neuronal degeneration induced by soluble oligomeric amyloid beta protein. *FASEB J* **17**:118–120.

52. Kim J-A, Mitsukawa K, Yamada MK, Nishiyama N, Matsuki N, Ikegaya Y (2002) Cytoskeleton disruption causes apoptotic degeneration of dentate granule cells in hippocampal slice cultures. *Neuropharmacology* **42**:1109–1118.

53. Krabbe G, Halle A, Matyash V, Rinnenthal JL, Eom GD, Bernhardt U *et al* (2013) Functional impairment of microglia coincides with Beta-amyloid deposition in mice with Alzheimer-like pathology. *PLoS ONE* **8**:e60921.

54. Kreutz S, Koch M, Böttger C, Ghadban C, Korf H-W, Dehghani F (2009) 2-Arachidonoylglycerol elicits neuroprotective effects on excitotoxically lesioned dentate gyrus granule cells via abnormal-cannabidiol-sensitive receptors on microglial cells. *Glia* **57**:286–294.

55. Kudo W, Lee H-P, Smith MA, Zhu X, Matsuyama S, Lee H-G (2012) Inhibition of Bax protects neuronal cells from oligomeric Aβ neurotoxicity. *Cell Death Dis* **3**:e309.

56. Kumamaru H, Saiwai H, Kobayakawa K, Kubota K, van Rooijen N, Inoue K *et al* (2012) Liposomal clodronate selectively eliminates microglia from primary astrocyte cultures. *J Neuroinflammation* **9**:116.

57. Lalancette-Hebert M, Gowing G, Simard A, Weng YC, Kriz J (2007) Selective ablation of proliferating microglial cells exacerbates ischemic injury in the brain. *J Neurosci* **27**:2596–2605.

58. Lee CYD, Landreth GE (2010) The role of microglia in amyloid clearance from the AD brain. *J Neural Transm (Vienna, Austria 1996)* **117**:949–960.

59. Lee JH, Won SM, Suh J, Son SJ, Moon GJ, Park UJ *et al* (2010) Induction of the unfolded protein response and cell death pathway in Alzheimer's disease, but not in aged Tg2576 mice. *Exp Mol Med* **42**:386–394.

60. Lue L-F, Kuo Y-M, Beach T, Walker DG (2010) Microglia activation and anti-inflammatory regulation in Alzheimer's disease. *Mol Neurobiol* **41**:115–128.

61. Lull ME, Block ML (2010) Microglial activation and chronic neurodegeneration. *Neurotherapeutics* **7**:354–365.

62. Maezawa I, Zimin PI, Wulff H, Jin L-W (2011) Amyloid-beta protein oligomer at low nanomolar concentrations activates microglia and induces microglial neurotoxicity. *J Biol Chem* **286**:3693–3706.

63. Malouf AT (1992) Effect of beta amyloid peptides on neurons in hippocampal slice cultures. *Neurobiol Aging* **13**:543–551.

64. Mandrekar S, Jiang Q, Lee CYD, Koenigsknecht-Talboo J, Holtzman DM, Landreth GE (2009) Microglia mediate the clearance of soluble Abeta through fluid phase macropinocytosis. *J Neurosci* **29**:4252–4262.

65. Masuch A, Shieh C-H, van Rooijen N, van Calker D, Biber K (2016) Mechanism of microglia neuroprotection: involvement of P2X7, TNFα, and valproic acid. *Glia* **64**:76–89.

66. Meyer-Luehmann M, Spires-Jones TL, Prada C, Garcia-Alloza M, de Calignon A, Rozkalne A *et al* (2008) Rapid appearance and local toxicity of amyloid-beta plaques in a mouse model of Alzheimer's disease. *Nature* **451**:720–724.

67. Minogue AM (2017) Role of infiltrating monocytes/macrophages in acute and chronic neuroinflammation: effects on cognition, learning and affective behaviour. *Prog Neuropsychopharmacol Biol Psychiatry* **79**:15–18.

68. Mosser DM (2003) The many faces of macrophage activation. *J Leukoc Biol* **73**:209–212.

69. Murgas P, Godoy B, von Bernhardi R (2012) Aβ potentiates inflammatory activation of glial cells induced by scavenger receptor ligands and inflammatory mediators in culture. *Neurotox Res* **22**:69–78.

70. Nakagawa T, Zhu H, Morishima N, Li E, Xu J, Yankner BA *et al* (2000) Caspase-12 mediates endoplasmic-reticulum-specific apoptosis and cytotoxicity by amyloid-beta. *Nature* **403**:98–103.

71. Neniskyte U, Neher JJ, Brown GC (2011) Neuronal death induced by nanomolar amyloid β is mediated by primary phagocytosis of neurons by microglia. *J Biol Chem* **286**:39904–39913.

72. Nimmerjahn A, Kirchhoff F, Helmchen F (2005) Resting microglial cells are highly dynamic surveillants of brain parenchyma in vivo. *Science (New York, N.Y.)* **308**:1314–1318.

73. Ridolfi E, Barone C, Scarpini E, Galimberti D (2013) The role of the innate immune system in Alzheimer's disease and frontotemporal lobar degeneration: an eye on microglia. *Clin Dev Immunol* **2013**:939786.

74. Roettger Y, Zerr I, Dodel R, Bach J-P (2013) Prion peptide uptake in microglial cells—the effect of naturally occurring autoantibodies against prion protein. *PLoS One* **8**:e67743.

75. Sai X, Kawamura Y, Kokame K, Yamaguchi H, Shiraishi H, Suzuki R *et al* (2002) Endoplasmic reticulum stress-inducible protein, Herp, enhances presenilin-mediated generation of amyloid beta-protein. *J Biol Chem* **277**:12915–12920.

76. Schultze JL (2015) Transcriptional programming of human macrophages: on the way to systems immunology. *J Mol Med* **93**:589–597.

77. Shadfar S, Hwang CJ, Lim M-S, Choi D-Y, Hong JT (2015) Involvement of inflammation in Alzheimer's disease pathogenesis and therapeutic potential of anti-inflammatory agents. *Arch Pharm Res* **38**:2106–2119.

78. Skibo GG, Nikonenko IR, Savchenko VL, McKanna JA (2000) Microglia in organotypic hippocampal slice culture and effects of hypoxia: ultrastructure and lipocortin-1 immunoreactivity. *Neuroscience* **96**:427–438.

79. Stoppini L, Buchs PA, Muller D (1991) A simple method for organotypic cultures of nervous tissue. *J Neurosci Methods* **37**:173–182.

80. Suh EC, Jung YJ, Kim YA, Park EM, Lee KE (2008) A beta 25–35 induces presynaptic changes in organotypic hippocampal slice cultures. *Neurotoxicology* **29**: 691–699.

81. Szalay G, Martinecz B, Lénárt N, Környei Z, Orsolits B, Judák L *et al* (2016) Microglia protect against brain injury and their selective elimination dysregulates neuronal network activity after stroke. *Nat Commun* **7**:11499.

82. Takahashi RH, Almeida CG, Kearney PF, Yu F, Lin MT, Milner TA *et al* (2004) Oligomerization of Alzheimer's beta-amyloid within processes and synapses of cultured neurons and brain. *J Neurosci* **24**:3592–3599.

83. Takata K, Kitamura Y, Yanagisawa D, Morikawa S, Morita M, Inubushi T *et al* (2007) Microglial transplantation increases amyloid-beta clearance in Alzheimer model rats. *FEBS Lett* **581**:475–478.

84. Tsay H-J, Huang Y-C, Huang F-L, Chen C-P, Tsai Y-C, Wang Y-H *et al* (2013) Amyloid β peptide-mediated neurotoxicity is attenuated by the proliferating microglia more potently than by the quiescent phenotype. *J Biomed Sci* **20**:78.

85. Turrin NP (2006) Tumor necrosis factor but not interleukin 1 mediates neuroprotection in response to acute nitric oxide excitotoxicity. *J Neurosci* **26**:143–151.

86. Umeda T, Tomiyama T, Sakama N, Tanaka S, Lambert MP, Klein WL *et al* (2011) Intraneuronal amyloid β oligomers cause cell death via endoplasmic reticulum stress, endosomal/lysosomal leakage, and mitochondrial dysfunction in vivo. *J Neurosci Res* **89**:1031–1042.

87. Vincent VAM, Selwood SP, Murphy Jr, GM (2002) Proinflammatory effects of M-CSF and A beta in hippocampal organotypic cultures. *Neurobiol Aging* **23**:349–362.

88. Vinet J, van Weering HRJ, Heinrich A, Kälin RE, Wegner A, Brouwer N *et al* (2012) Neuroprotective function for ramified microglia in hippocampal excitotoxicity. *J Neuroinflammation* **9**:27.

89. Wang X, Takata T, Sakurai T, Yokono K (2007) Different effects of monocarboxylates on neuronal survival and beta-amyloid toxicity. *Eur J Neuorsci* **26**:2142–2150.

90. Wisniewski ML, Hwang J, Bahr BA (2011) Submicromolar Aβ42 reduces hippocampal glutamate receptors and presynaptic markers in an aggregation-dependent manner. *Biochem Biophys Acta* **1812**:1664–1674.

91. Wolf SA, Boddeke HWGM, Kettenmann H (2017) Microglia in physiology and disease. *Annu Rev Physiol* **79**:619–643.

92. Wyss-Coray T, Rogers J (2012) Inflammation in Alzheimer disease-a brief review of the basic science and clinical literature. *Cold Spring Harb Perspect Med* **2**:a006346.

93. Yang T, Knowles JK, Lu Q, Zhang H, Arancio O, Moore LA *et al* (2008) Small molecule, non-peptide p75 ligands inhibit Abeta-induced neurodegeneration and synaptic impairment. *PLoS One* **3**:e3604.

94. Yu Z, Luo H, Fu W, Mattson MP (1999) The endoplasmic reticulum stress-responsive protein GRP78 protects neurons against excitotoxicity and apoptosis: suppression of oxidative stress and stabilization of calcium homeostasis. *Exp Neurol* **155**:302–314.